Clinical and Translational Imaging (2024) 12:55–68
https://doi.org/10.1007/s40336-023-00595-z

EXPERT REVIEW

Multimodality imaging for diagnosis, risk stratification, and treatment monitoring of cardiac sarcoidosis

Kathleen A. Young[1] · Tristan Raoult[2] · Lucia Leccisotti[3] · Bernhard L. Gerber[2] · Panithaya Chareonthaitawee[1] · Olivier Gheysens[4]

Received: 13 July 2023 / Accepted: 30 August 2023 / Published online: 26 September 2023

Abstract

Cardiac sarcoidosis (CS), with either extracardiac involvement or in isolation, is increasingly recognized. Complications from cardiac involvement are the leading cause of death in patients with sarcoidosis, rendering early detection extremely important given the significant therapeutic and prognostic implications. However, the diagnosis of CS remains challenging due to the lack of a reliable gold standard, largely due to the low sensitivity of traditional endomyocardial biopsy and patchy myocardial involvement. Recent advances in cardiac imaging with [18F] fluorodeoxyglucose positron emission tomography–computed tomography ([18F]FDG PET/CT) and cardiac magnetic resonance (CMR) have provided unprecedented information on the prevalence of CS and have revolutionized the diagnosis and management of CS patients. Abnormal PET/CMR findings are now major criteria in societal guidelines to establish a probabilistic diagnosis of CS. This review provides a brief introduction to CS and a summary of current diagnostic criteria, followed by a review on the current use and strengths of PET/CT and CMR for diagnosis, risk stratification, and treatment response evaluation. CMR is the most robust technique to assess left ventricular function, to detect myocardial fibrosis, and differentiate CS from other cardiomyopathies and has an excellent negative predictive value. On the other hand, [18F]FDG PET/CT is the modality of choice to assess active myocardial inflammation which may be amenable to immunosuppressive treatment as well as to detect extracardiac involvement, to identify potential biopsy sites, and to monitor treatment efficacy. Understanding the complementary value of both techniques is crucial to the optimal utilization of advanced imaging in patients with CS. Lastly, some gaps are identified for future research.

Keywords Cardiac sarcoidosis · Fluorodeoxyglucose · Positron emission tomography · PET/CT · Cardiac magnetic resonance imaging

Introduction

Sarcoidosis is a systemic disease characterized by non-caseating granulomatous inflammation, most commonly involving the lungs or lymph nodes [1]. However, the incidence of cardiac sarcoidosis (CS), that may occur with extracardiac involvement or rarely in isolation, has been increasingly recognized [2]. This trend is corroborated in a Finnish cohort study that reported an exponential increase from 1988 to 2012 with a prevalence of 2.2 per 100,000 adults [3] and an estimated prevalence of 10–40/100,000 adults in Europe and the United States [4]. Among patients with systemic disease, the minority (5%) will have clinical manifestations of CS such as cardiomyopathy, arrhythmia, or atrioventricular conduction disturbances. By contrast, more than 25% may have evidence of cardiac involvement on autopsy, [5] and this

Panithaya Chareonthaitawee and Olivier Gheysens share authorship.

✉ Panithaya Chareonthaitawee
Chareonthaitawee.panithaya@mayo.edu

[1] Department of Cardiovascular Medicine, Mayo Clinic, 200 First St SW, Rochester, MN 55905, USA

[2] Division of Cardiology, Department of Cardiovascular Diseases, Cliniques Universitaires St. Luc and Pole de Recherche Cardiovasculaire (CARD), Institut de Recherche Expérimentale et Clinique (IREC), UCLouvain, Ottignies-Louvain-la-Neuve, Belgium

[3] Section of Nuclear Medicine, Università Cattolica del Sacro Cuore and Fondazione Policlinico Universitario A. Gemelli IRCCS, Rome, Italy

[4] Department of Nuclear Medicine, Cliniques Universitaires Saint-Luc, Université Catholique de Louvain, Brussels, Belgium

figure increases up to 30% with modern imaging techniques [6–8]. The prevalence of isolated CS is estimated to be up to 20% and is underrecognized [9]. Complications from cardiac involvement remain the leading cause of death in patients with sarcoidosis, rendering early detection critical given the significant therapeutic and prognostic implications. Recent advances in cardiac imaging have revolutionized the diagnosis and management of CS patients, even though no single imaging modality is diagnostic for the disease. Cardiac magnetic resonance imaging (CMR) allows visualization of focal areas of fibrosis in a non-coronary distribution, while [18F]-fluorodeoxyglucose ([18F]FDG) positron emission tomography–computed tomography (PET/CT) provides valuable insights into areas of active inflammation. The presence of inflammation is particularly relevant as it signifies active disease that may be treated with immunosuppressive therapy, and inflammation likely precedes the development of irreversible fibrosis, though inflammation and scar may co-exist in the same heart. This comprehensive review explores the role of modern advanced imaging techniques, such as PET and CMR, for the detection, risk stratification, and monitoring of CS.

Diagnostic criteria for CS

The diagnosis of CS and its differentiation from other infiltrative and inflammatory cardiomyopathies and in particular giant cell myocarditis remain challenging due to the lack of a reliable gold standard. Histological confirmation by endomyocardial biopsy (EMB) has a low sensitivity (20–30%) because of the focal/patchy nature of the disease with large inter-patient variability and sub-epicardial predilection [10]. In addition, EMB is an invasive procedure with potentially severe though uncommon complications. On the other hand, modern imaging techniques have an overall high sensitivity but lack specificity for diagnosing CS. To address these limitations, societal guidelines have been developed to establish the diagnosis of CS on a probability basis using a combination of histopathological, clinical, and imaging findings (Table 1). The two most commonly used guidelines are those of the Heart Rhythm Society (HRS) and the Japanese Circulation Society (JCS). These guidelines use a combination of clinical and imaging findings, as well as histologic evidence of extracardiac disease to diagnose 'probable' CS. While the JCS accepts a clinical diagnosis of extracardiac sarcoidosis, the HRS criteria do not. More recently, an additional 'presumed' diagnostic category was proposed, in which clinical and imaging evidence suffice to make the diagnosis of CS in the absence of any histopathological proof [11].

The absence of sarcoidosis outside of the heart does not rule out the potential for sarcoidosis specifically affecting the heart. By definition, isolated CS can only be diagnosed in the setting of no clinical findings of sarcoidosis in any other organ, and therefore the aforementioned clinical diagnostic pathways cannot be utilized. The updated Japanese guidelines now provide a list of criteria to establish the diagnosis of isolated CS which may be done by histologic diagnosis on EMB or surgical specimen or clinically based on cardiac [18F]FDG uptake plus additional clinical criteria [12].

PET and CMR for diagnosing cardiac sarcoidosis

PET

PET is a valuable non-invasive diagnostic technique for detecting and quantifying radiopharmaceutical accumulation in tissues, playing a crucial role in the multimodality approach to diagnosing CS. PET is currently the most robust imaging method for assessing disease activity both within and beyond the heart. PET-CT is nowadays the standard, allowing precise co-localization of metabolic abnormalities and anatomic structures, facilitating diagnosis, disease activity assessment, treatment response monitoring, and guiding biopsies in cardiac and extracardiac sarcoidosis. While PET/MR scanners also enable simultaneous evaluation of myocardial structure, function, and tissue characterization, their availability remains limited.

The recommended radionuclide method for comprehensive evaluation of CS is assessing both myocardial perfusion and inflammation using [18F]FDG [13–15]. This approach acknowledges that perfusion defects in CS can signify inflammation, scarring, or a combination of both, whereas abnormal [18F]FDG uptake indicates inflammation. Given the potential coexistence of inflammation and scarring, patients may exhibit various patterns of perfusion and metabolism abnormalities.

Unlike coronary artery disease, CS does not typically exhibit myocardial perfusion defects following a coronary artery distribution. These perfusion defects can be related to either external microvascular compression from granulomas and/or inflammation or may result from fibrotic scarring. In the active stage, some perfusion defects may be reversible with immunosuppressive therapy, while in the chronic phase, irreversible perfusion defects may be present and may be accompanied by regional wall motion abnormalities as fibrosis replaces granulomas.

[18F]FDG PET can detect the presence, intensity, and extent of disease activity, i.e., inflammation, in cardiac and extracardiac sarcoidosis. [18F]FDG is a glucose analog and its uptake reflects the glycolytic activity. The high glycolytic activity of inflammatory cells, such as activated macrophages and CD4+ T lymphocytes, explains the intense

Table 1 Diagnostic criteria for CS

	Heart Rhythm Society (2014)	Japanese Circulation Society (2017)	
		Cardiac sarcoidosis	Isolated Cardiac Sarcoidosis
Histological diagnosis	Non-caseating granulomas on histological examination of myocardial tissue with no alternative cause	Non-caseating granulomas on EMB or surgical specimen	Non-caseating granulomas on EMB or surgical specimen
Clinical diagnosis	Histologic diagnosis of extracardiac sarcoidosis, and ≥ 1 clinical criteria, and other causes have been reasonably excluded = « probable » cardiac sarcoidosis	Histologic extracardiac sarcoid (or clinical pulmonary/ophthalmic sarcoidosis and ≥ 2 laboratory criteria), and ≥ 2 major criteria or 1 major and ≥ 2 minor criteria	Prerequisite No clinical findings characteristic of extracardiac sarcoidosis No extracardiac abnormal accumulation of ^{67}Ga or FDG Chest CT : no shadow along lymphatic tracts in lungs or no lymphadenopathy (minor axis > 10 mm) High myocardial ^{67}Ga or FDG uptake in the myocardium AND ≥ 3 other major criteria
Clinical criteria	Cardiomyopathy or heart block responsive to steroid ± immunosuppressive treatment Mobitz type II 2nd degree heart block or 3rd degree heart block Unexplained reduced LVEF < 40% Unexplained sustained (spontaneous or induced) VT Positive ^{67}Ga uptake in a pattern consistent with CS LGE on CMR in a pattern consistent with CS Patchy uptake on FDG PET in a pattern consistent with CS	**Major** High-grade AV block or sustained VT/VF Basal/mid septal thinning or abnormal wall anatomy LVEF < 50% High myocardial ^{67}Ga or FDG uptake in the myocardium LGE on CMR **Minor** Abnormal ECG findings : bundle branch block, axis deviation, Q waves, ventricular arrhythmias Perfusion defects on myocardial perfusion scintigraphy EMB : monocyte infiltration and ≥ moderate interstitial fibrosis	**Major** High-grade AV block or sustained VT/VF Basal/mid septal thinning or abnormal wall anatomy LVEF < 50% High myocardial ^{67}Ga or FDG uptake in the myocardium LGE on CMR
Laboratory criteria	Not applicable	Bilateral hilar lymphadenopathy High serum ACE activity or elevated serum lysozyme levels High serum soluble interleukin-2 receptor (sIL-2R) levels Significant tracer accumulation in ^{67}Ga scintigraphy or FDG PET High percentage of lymphocytes with CD4/CD8 ratio of > 3.5 in BAL fluid	

ACE, angiotensin-converting enzyme; AV, atrioventricular; BAL, bronchoalveolar lavage; CS, cardiac sarcoidosis; CMR, cardiac magnetic resonance; EMB, endomyocaridal biopsy; ^{67}Ga, gallium-67 citrate; FDG PET, fluorodeoxyglucose positron emission tomography; LGE, late-gadolinium enhancement; LVEF, left ventricular ejection fraction; VT/VF, ventricular tachycardia/fibrillation

Japanese Circulation Society guidelines from Terasaki et al.

Heart Rhythm Society criteria from Birnie et al.

[18F]FDG uptake in active granulomatous sarcoid lesions [16, 17]. However, myocardial assessment by [18F]FDG PET is complex due to the physiological glucose uptake by normal myocardial cells. Achieving proper suppression of myocardial glucose uptake is crucial to unmask active cardiac sarcoid lesions, and a combination of prolonged fasting and dietary manipulation appears to be the most effective preparation method. While the European Association of Nuclear Medicine (EANM) guidelines recommend a strict high-fat, carbohydrate-free diet for 12–24 h combined with a prolonged fasting of 12–18 h prior to [18F]FDG administration, the Joint Society of Nuclear Medicine and Molecular Imaging—American Society of Nuclear Cardiology (SNMMI-ASNC) expert consensus document suggests at least two high-fat (> 35 g), low-carbohydrate (< 3 g) meals the day before the study followed by fasting for 4–12 h. Intravenous unfractionated heparin (50 IU/kg approximately 15 min prior to [18F]FDG injection) may be used in conjunction with the high-fat, low-carbohydrate diet and prolonged fasting [9, 13, 18]. Although prolonged fasting (> 18 h) alone is an alternative option recommended by SNMMI and ASNC, it appears to be less effective for myocardial suppression of physiologic glucose uptake than the combined approaches and should be avoided as much as possible based on clinical experience. Exercise and myocardial ischemia may increase myocardial [18F]FDG uptake. It is, therefore, important to avoid intense exercise or stress testing for at least 12 h before the PET scan, and patients should continue to fast and remain physically inactive until the end of PET imaging. Despite various dietary recommendations, physiological myocardial [18F]FDG uptake may still be observed in up to 20% of patients.[9] Some practices have extended patient preparation to include 2 to 3 days of high-fat, low-carbohydrate meals along with multiple overnight fasts based on recent studies [19].

Extensive literature is available on camera acquisition, data reconstruction, and data analysis for CS assessment using PET [9, 13, 18]. The recommended protocol involves performing resting myocardial perfusion imaging with [13N]NH3 or 82Rb, followed by a non-gated cardiac acquisition 60–90 min after intravenous administration of [18F]FDG [13, 20]. If PET myocardial perfusion imaging is unavailable, SPECT with 201Tl or [99mTc]-labeled radiotracers may be used, preferably with attenuation correction. Gated perfusion images permit assessment of left ventricular (LV) global and regional contractile function, providing important diagnostic and prognostic information. The addition of phase analysis to gated-PET resulted in improved detection of scar related to CS, superior to perfusion assessment alone [21]. The potential added value of quantification of myocardial blood flow and coronary flow reserve by PET in the diagnosis of CS has been explored in one study and remains to be further investigated [22]. Lastly, whole body [18F]FDG imaging can be considered for assessment of extracardiac disease activity (lung, lymph nodes, liver, spleen, kidneys, and bones) in the same session. This is strongly recommended at the time of the patient's initial cardiac scan particularly if there is no prior diagnosis of sarcoidosis, to identify other organs of involvement and possible extracardiac biopsy sites.

The interpretation of PET for CS may be challenging and requires a comprehensive evaluation of all the available data, including consideration of non-sarcoid causes of myocardial perfusion and [18F]FDG abnormalities as well as the integration with other imaging findings. Image interpretation begins with a quality-control assessment, including confirmation of proper co-registration between CT and PET images and confirmation of adequate suppression of physiological myocardial [18F]FDG uptake, defined as myocardial [18F]FDG uptake lower than that of the blood pool. Interpretation of PET images for CS is based on the use of traditional nuclear cardiology display systems with both rest myocardial perfusion and [18F]FDG images displayed simultaneously according to the standard cardiac axes with image intensity normalized to maximum counts per pixel of the respective data set. The use of resting myocardial perfusion imaging in association with [18F]FDG PET is particularly helpful not only for visual image interpretation but also for the orientation of [18F]FDG images themselves, especially when only focal [18F]FDG uptake is present. The combined assessment of perfusion and inflammation allows visualization of the full spectrum of CS disease from "pure inflammation" ([18F]FDG positive without perfusion abnormality) to "fibrosis-predominant" (perfusion defect without [18F]FDG uptake) through the intermediate stages (varying degrees of both inflammation and fibrosis) [13]. A representative example of inflammation with concomitant decreased perfusion is shown in Fig. 1.

Resting myocardial perfusion images are classified as normal or abnormal, with regional myocardial perfusion defect(s) described as mild, moderate, severe, or absent taking into account location and extent. It is important to exercise caution when interpreting [13N]NH3 images as mild perfusion abnormalities of the LV lateral wall may be a normal variant.

Qualitatively, [18F]FDG uptake can be described as absent, focal, diffuse, or focal on diffuse. Focal and focal on diffuse [18F]FDG uptake are suggestive of CS, whereas diffuse uptake is usually due to suboptimal patient preparation rather than diffuse CS. Sarcoid lesions are typically localized

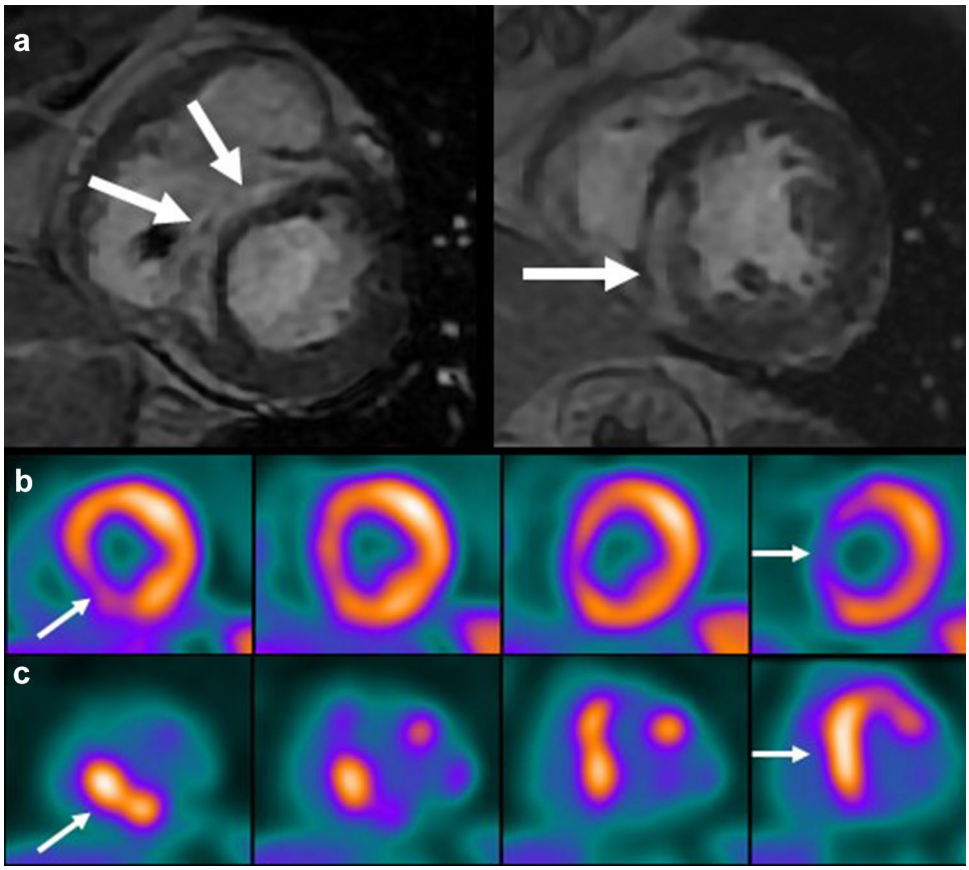

Fig. 1 A 65 year-old female with history of high-grade AV block (treated with dual chamber pacemaker and His bundle pacing), hypertension and Sjogren's presented with progressive dyspnea and fatigue. Chest CT showed mediastinal and cervical lymphadenopathies and biopsy of a submandibular lymph node confirmed the diagnosis of extracardiac sarcoidosis. Given the cardiac manifestation, CMR (**a**) was performed and showed areas of sub-epicardial late-gadolinium enhancement of the basal to midventricular septum. [18F]FDG PET was obtained to assess for active inflammation (**b**), (**c**) with 13N-ammonia perfusion (**b**), and FDG imaging (**c**) showing matched predominantly septal perfusion defect with focal FDG uptake establishing the diagnosis of probable active cardiac sarcoidosis

at the basal segments, especially the septum or lateral wall of the LV. The presence of focal or focal on diffuse [18F] FDG uptake and a matched perfusion defect in the same area is strongly suggestive of active CS, in the absence of other causes. The presence of myocardial [18F]FDG uptake on the normalized cardiac display should be confirmed on the general nuclear medicine display because the normalization can lead to accentuation of areas of mild [18F]FDG uptake. It is important to note that [18F]FDG uptake in the LV lateral wall without perfusion defect or any other imaging findings such as echocardiographic wall motion abnormalities or cardiac MRI findings may be a non-specific finding. In addition, both corrected and non-corrected PET images should be evaluated in patients with intra-cardiac devices because CT-attenuation correction may result in false positive [18F] FDG uptake around device leads.

In addition to the assessment of the LV, it is important to look for areas of focal [18F]FDG uptake in the right ventricle. The latter is more reliable for the diagnosis of CS because physiological [18F]FDG uptake is less frequently observed than in the LV. [18F]FDG uptake by the right ventricle is associated with an increased risk of cardiac events and serves as a marker of disease severity [23].

PET imaging for CS is associated with several potential pitfalls. These include false positive [18F]FDG uptake due to suboptimal patient preparation, patient motion, metal and calcification artifacts or other conditions (e.g., tumor, myocarditis, hibernating myocardium, arrhythmogenic cardiomyopathy, amyloidosis, hypertrophic cardiomyopathy, systemic rheumatologic diseases associated with myocardial inflammation, papillary muscle uptake, and right ventricular uptake due to pulmonary hypertension) [24].

Inflammatory activity using PET can also be quantitatively analyzed using various metrics. These include SUVmax, the average SUV in 17 myocardial segments (SUVmean), the sum of SUVs of all myocardial segments (SUVtotal), the heart-to-blood pool SUV ratio (cardiac SUVmax/blood pool SUVmax), the coefficient of variance of SUVs (a measure of inflammation heterogeneity), the sum of voxels with SUVs above liver or blood pool uptake (total cardiac metabolic volume, tCMV), the product of the CMV by the mean SUV of the involved tissue (total cardiac metabolic activity, tCMA), and the product of the maximum SUV in the left ventricle and the number of segments with abnormal uptake (myocardial uptake index, UI) that measure the extent and severity of [18F]FDG uptake [23, 25–35]. These methods have not been compared head-to-head, nor correlated with outcomes in large studies but seem to perform better than visual analysis mainly to predict or assess treatment response [32, 33, 35]. Moreover, new PET scanners with high temporal and spatial resolution can improve the detection of CS, allowing a more detailed evaluation of radiotracer distribution for the analysis of textural features of [18F]FDG PET images [36–39].

CMR

CMR is a valuable imaging modality for detecting cardiac involvement in patients with sarcoidosis. Its value lies not only in its high sensitivity and ability to identify other alternative cardiac diseases that may account for a patient's clinical presentation, but also in the fact that CMR detection of sarcoid involvement is associated with significantly worse prognosis.

CMR allows for a comprehensive evaluation of patients with suspected CS. Recommended imaging protocols include (1) CINE images in multiple planes including a stack of LV short axis images covering the whole heart and additional long-axis sections (2, 3, and 4 chambers and right ventricular long-axis views) for left and right ventricular (RV) volumes and function, (2) T2 imaging, T1 and T2 mapping for evaluation of inflammation and (3) late-gadolinium imaging. Images are generally acquired during breath-holds; however, it is possible for patients with difficulties holding their breath to use real-time cardiac sequences. CMR is now also feasible in patients with devices such as pacemakers and implantable cardioverter defibrillator (ICD), since most current devices are now MR compatible and new sequences such as wideband late-gadolinium enhancement (LGE) are less artifact prone.

CS is often associated with reduced cardiac function and CMR provides an accurate and reproducible assessment of LV and RV volumes and function. Both guidelines from the JCS and the HRS consider a decrease in LV ejection fraction (LVEF) as a major criterion for diagnosing CS (Table 1). However, they differ on the threshold, with the JCS requiring only a decrease below 50%, whereas HRS considers LVEF below 40% [40]. Cine imaging sequences on CMR are very accurate for the detection of ventricular aneurysms, pericardial effusion, and valve pathology [41, 42]. These imaging sequences are especially useful in CS for evaluation of regional ventricular dysfunction, increased wall thickness or thinning, and assessment of right ventricular function and wall motion [43]. Right ventricular dysfunction can be due to right ventricular infiltration by granulomas but also be secondary to right ventricular pressure overload in the setting of pulmonary hypertension in pulmonary sarcoidosis.

The principal value for detecting CS by CMR relies on identifying typical patterns of LGE. Because of its high spatial resolution, CMR can detect very small areas of LGE in suspected CS, contributing to its high sensitivity. Interestingly, small areas of LGE are often not associated with any ECG or echocardiographic abnormalities. Gadolinium (Gd)-based contrast agents are very safe with few side effects but should be used with care in patients with significant renal impairment (eGFR < 30 ml/min) [44]. The underlying principles of delayed enhancement imaging rely on the fact that Gd-based contrast agents have extracellular distribution volume and will accumulate in areas of fibrosis and inflammation within a few minutes after intravenous administration. The presence of LGE is non-specific as it may occur in many different cardiac disorders, including myocarditis, cardiomyopathy, cardiac neoplasms, and genetic diseases. However, differential diagnosis is offered by the patterns of LGE, which are relatively disease specific. Typical patterns that strongly suggest the diagnosis of CS include mid-wall and sub-epicardial, multifocal LGE that do not correspond to coronary artery distribution territories. In addition, LGE involvement of the basal septum, as well as contiguous extension into the right ventricle (the so-called hook sign) are commonly seen in CS [7]. Figure 1 illustrates a typical septal involvement on LGE. However, other patterns may also occur, mimicking those of many other cardiac diseases. Indeed, CS can sometimes be associated with sub-endocardial LGE, mimicking an infarct pattern. On the other hand, it is uncommon to see isolated LV transmural involvement, absence of septal involvement, or isolated involvement of only one LV level [45]. Lack of gross LV myocardial involvement or isolated sub-endocardial LGE should prompt the search for an alternative diagnosis. Unfortunately, because of the wide range of patterns in sarcoidosis, the identification of LGE patterns may be not specific. In particular, patterns in CS and giant cell myocarditis are identical, making it

impossible to qualitatively distinguish the two entities [46]. The presence of LGE reflects both fibrotic scar and active inflammation due to granulomas, and therefore LGE is not always irreversible but may regress during treatment. The extent of LGE is, however, closely associated with disease severity and reduction of LVEF [47].

T1 and T2 mappings allow for additional information in patients with CS. T1 mapping allows assessment of early and diffuse myocardial tissue abnormalities not visible on LGE sequences [48, 49] while increased T2-weighted signal reflects increased water in the setting of active inflammation [50]. Since these changes may be small, quantitative T1 and T2 mapping are considered more sensitive than T2-weighted imaging in the recognition of myocardial inflammation in CS. As compared to healthy subjects, patients with sarcoidosis have often significantly higher native T1, T2, and extracellular volumes. Interestingly, those changes are observed even in patients with subclinical CS and without LGE findings [51]. These techniques may be challenging in the setting of frequent ectopy, which may be observed in patients referred for imaging for CS.

It is unclear if, and when, a negative CMR should be repeated. The HRS guideline recommends monitoring symptoms, ECG, and echocardiogram among patients with extracardiac sarcoidosis and previously normal CMR. Repeated imaging should be considered in cases of clinical changes. In patients with a negative CMR where there is high suspicion for CS, cardiac PET should be considered [52].

Diagnostic accuracy

Several studies have evaluated the diagnostic accuracy of PET for CS, with reported high sensitivity but lower specificity. Sensitivity of [18F]FDG PET/CT for CS diagnosis ranges from 27 to 100%, while specificity ranges from 33 to 100% [53–55]. Combined myocardial perfusion imaging and [18F]FDG PET showed slightly higher diagnostic accuracy than [18F]FDG PET without perfusion imaging (78% vs. 75% sensitivity and 87% vs. 83% specificity, respectively), though differences did not reach statistical significance [56]. The wide range of estimates can be attributed to study heterogeneity, including variable sample sizes, different populations, retrospective designs, diverse preparation and imaging protocols, and the choice of reference standard for CS. Additionally, the use of the older guidelines as reference standards may have led to misclassification or limited detection of patients with early-stage subclinical CS lesions and/or isolated CS.

For CMR, a meta-analysis of eight studies ($n = 649$) assessing the diagnostic accuracy for CS showed an overall sensitivity of 93% (95% CI 0.87–0.97) and specificity of 85% (95% CI 0.68–0.94) [57]. A subgroup analysis with only studies performed between 2011 and 2017 yielded a similar sensitivity of 95% (95% CI 0.88–0.98) but improved specificity of 92% (95% CI 0.49–0.99).

Recently, Aitken and colleagues performed a systematic review and meta-analysis to compare the diagnostic accuracy of CMR and [18F]FDG PET for CS [58]. In the analysis restricted to the subgroup of 6 studies (303 patients) with direct comparison of CMR and PET in the same patients, CMR had a mean sensitivity of 92% (95% CI: 0.82–0.96) and mean specificity of 72% (95% CI: 0.40–0.91) while PET had a sensitivity of 81% (95% CI: 0.57–0.93) and specificity of 82% (95% CI: 0.58–0.94). In addition, sensitivity of [18F]FDG PET was significantly higher with quantitative evaluation compared with qualitative assessment (93% vs. 76%; $P = 0.01$), whereas specificity did not differ. However, [18F]FDG PET results were interpreted in combination with myocardial perfusion imaging in only one out of six studies included.

Treatment response

Cardiac [18F]FDG PET is considered the imaging modality of choice to monitor and quantify treatment response in patients with CS (Figs. 2, 3). Several PET parameters have been proposed of which SUVmax and tCMA correlated best with improvement on serial imaging [32, 33]. For example, Osborne et al. showed that a mean decrease in SUVmax of 10 g/ml inversely correlated with an improvement of LVEF of 7.9% in CS patients treated with steroids. However, there is no universal consensus on the cutoff value to define response on [18F]FDG PET. The SNMMI/ASNC consensus document defines response as a concordant decrease in tCMA and SUVmax of at least 20% [34]. It is important to consider that quantitative parameters hold validity only when there is uniformity throughout the entire imaging procedure, including patient preparation, across serial scans. To date, it is unknown whether a decrease in [18F]FDG uptake is associated with a reduction in major events or whether ICD implantation can be delayed or avoided in patients with active disease before fibrosis or LV dysfunction occurs. In a small observational study, the use of serial [18F]FDG PET was shown to be beneficial in guiding immunosuppressive therapy in patients with CS and resulted in low chronic steroid doses and satisfactory disease control at 1 year [59].

Using CMR for monitoring treatment response instead of [18F]FDG PET offers the benefit of avoiding ionizing radiation exposure, which may be particularly relevant in this younger population. However, while the value of LGE in the diagnosis of CS is well established, little is known about serial LGE assessment for the evaluation of treatment response in CS. In a study which utilized a qualitative evaluation of LGE sequences, six patients, including three

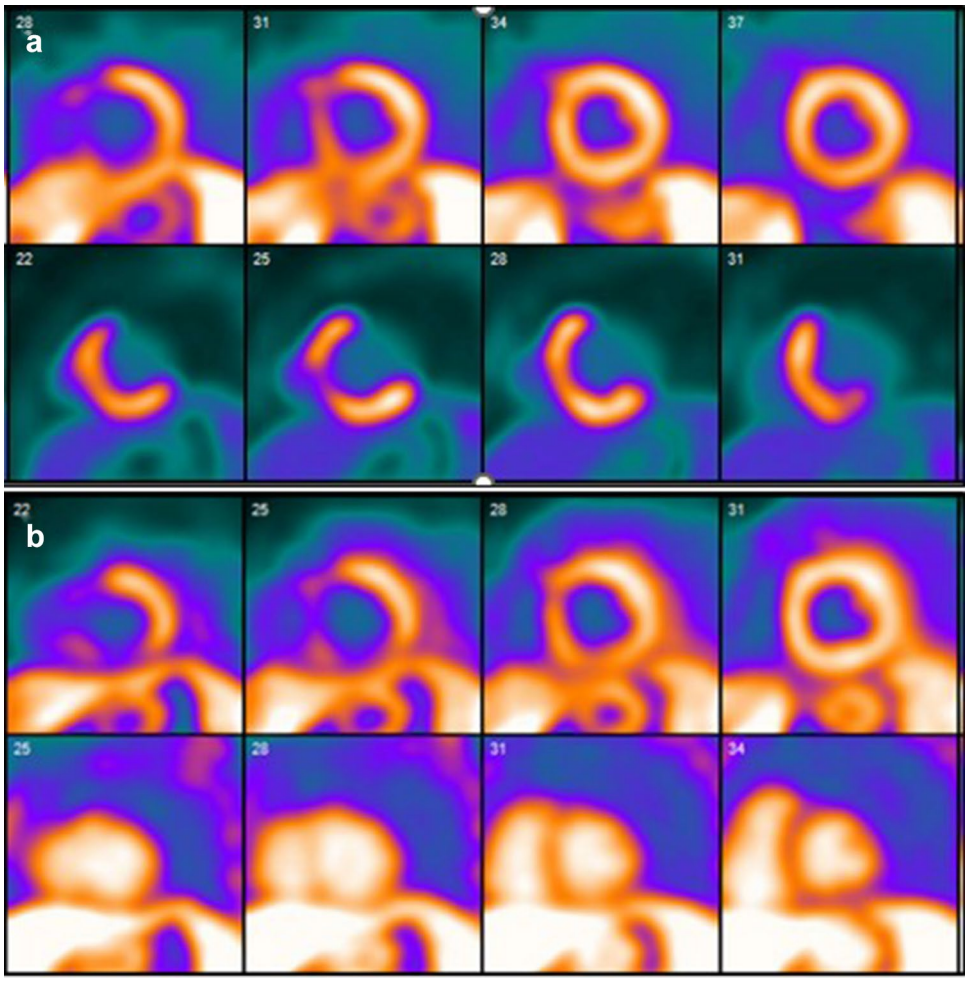

Fig. 2 A 66 year-old female with frequent symptomatic PVCs, non-sustained ventricular tachycardia, and first-degree atrioventricular block. Due to abnormal perfusion stress imaging, she underwent coronary angiogram which showed non-obstructive coronary artery disease. Subsequent cardiac MRI showed concern for both left ventricular delayed enhancement in a pattern consistent with cardiac sarcoidosis. Pulmonary lymph node biopsy was positive for sarcoidosis. Panel **a** demonstrates initial [18F]FDG PET scan which shows marked 13N-ammonia perfusion defect (top row) with matched FDG uptake (bottom row). Maximum myocardial standard uptake value (SUV) was 10.1, maximum blood pool 1.8. She was initiated on standard immunosuppressive regimen. Panel **b** is her follow-up scan 6 months later which shows persistent perfusion defects (top row), but FDG uptake had largely resolved (bottom row). Maximum myocardial SUV—2.7, maximum blood pool SUV—2.3

with clinical cardiac involvement, treated with high-dose steroids, had resolution or improvement of LGE at their 12-month CMR follow-up [60]. Recently, quantifying LGE has emerged as an objective method for measuring myocardial scar, with various approaches described in the literature [61]. Ise et al. [62] reported that patients with a large extent of LGE ($\geq$ 20% using a definition of signal threshold 5 standard deviations above the signal intensity of normal myocardium) were less likely to have improvement in LVEF at 6 months following corticosteroid therapy.

T1 and T2 quantitative measures have the potential to track changes in patients undergoing treatment for CS, such as reflecting decreased inflammation from immunosuppressive therapy and/or positive remodeling effects of guideline-directed medical therapy. One study has demonstrated a reduction of native of T1 and T2 values to anti-inflammatory therapy [63]. However, further studies are required to determine the role of T1 and T2 mapping in assessing treatment response in CS patients.

Lastly, CMR strain imaging is an emerging topic with potential application in the early identification and treatment response of patients with CS. However, initial results in identifying cardiac abnormalities in patients with systemic sarcoidosis have been mixed [64, 65] and its use in following treatment response is limited to case reports [66]. Further validation in this patient population is needed.

To date, neither randomized controlled trials nor formal recommendations are available on the optimal timing of serial imaging in patients with CS. Our approach is to bring patients back for the first return for repeat [18F] FDG PET/CT after 3–6 months. Following that initial return, patients may come back on an annual basis with or without [18F]FDG PET based on their overall clinical status. In the absence of evidence, the imaging interval is often determined by the treating physician taking into account the disease extent and severity on baseline imaging as well as the patient's clinical evolution.

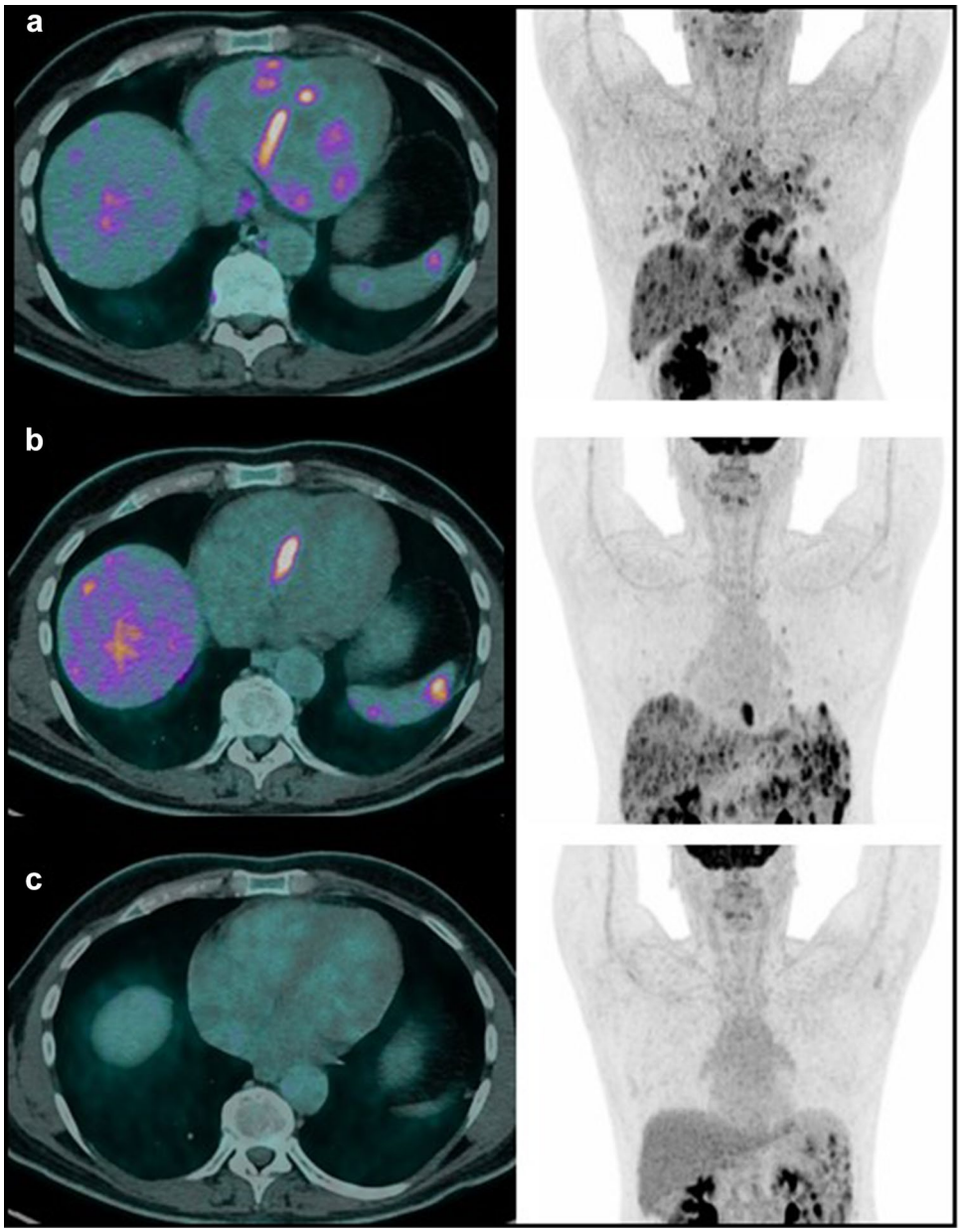

Fig. 3 A 61-year-old male with biopsy proven sarcoidosis underwent whole body [18F]FDG PET/CT showing multiple foci of intense [18F]FDG uptake in lymph nodes, lungs, liver, spleen, right and left ventricle compatible with multiorgan involvement (**a**). Treatment with prednisone and methotrexate was initiated and [18F]FDG PET/CT 12 months later showed partial metabolic response with persistent multiorgan involvement including active myocardial disease (**b**). Prednisone was tapered and infliximab was added to methotrexate. Subsequent [18F]FDG PET/CT 12 months after treatment modification showed complete metabolic response (**c**)

Risk stratification

LGE on CMR is one of the strongest prognostic markers in CS, with a significantly increased risk for both ventricular arrhythmia (odds ratio 20.3) and all-cause mortality (odds ratio 3.45) in patients with LGE, based on a recent meta-analysis [67]. In addition, another recent meta-analysis including 899 patients showed that CS patients with RV LGE have a significantly higher risk for composite events and sudden cardiac death compared to patients without RV LGE [68]. Conversely, the absence of LGE portends an excellent event-free survival.

Both qualitative and quantitative [18F]FDG PET findings have a prognostic value in CS. In a single-center study including 203 patients, quantitative assessment of the extent and severity of perfusion-metabolism mismatch and coefficient of variation of [18F]FDG uptake was associated with adverse outcome [23]. The combination of abnormal [18F]FDG uptake with a perfusion defect was found to have a fourfold higher risk of ventricular arrhythmia or death [25]. Similar to RV LGE, pathological [18F]FDG uptake in the RV wall is strongly associated with adverse cardiovascular events, highlighting the importance of assessing the RV during imaging review [25, 69, 70].

Even though both [18F]FDG PET and CMR have prognostic value in CS patients, CMR has been shown to be superior in predicting major cardiac events in an analysis of 5 studies comparing MRI and PET in 276 patients [58].

Patients with CS with significant conduction system disease will require a permanent pacemaker. Whether all patients diagnosed with CS with and without conduction system disease should receive an ICD is controversial. Current ESC guidelines indicate ICD implantation for primary prevention in all patients with CS and LVEF < 35% as class I indication with level of evidence B in, and in patients with LVEF > 35% with significant LGE after resolution of acute inflammation as Class IIa indication with a level of evidence B [71]. They propose electrophysiological study for risk stratification in patients with LVEF 35–50% and minor LGE after resolution of acute inflammation (Class IIa level of evidence C). In contrast, the 2017 AHA/ACC/HRS guidelines recommend ICD implantation for primary prevention in patients with CS and LVEF < 35% (class I) and in patients with CS with any evidence of myocardial scar by CMR or cardiac PET/CT (class IIa indication) [72]. However, Elwazir et al. recently demonstrated a low sensitivity for detection of myocardial scar by cardiac PET/CT compared to CMR [21], and in clinical practice assessment of myocardial scar is most commonly completed with CMR. One study identified an optimal cutoff for myocardial LGE of > 5.7% for the prediction of sudden cardiac death or ventricular arrhythmias [73]. Another study described that certain CMR phenotypes in CS are associated with an increased risk of arrhythmias and heart failure, which could also help optimize the identification of patients best served by ICD placement [74].

Complementary value of PET and CMR

Multimodality imaging remains crucial for diagnosing and managing CS. While awaiting the widespread integration of hybrid PET/MR imaging, which combines the advantages of each modality, the question often arises regarding the optimal initial diagnostic test for evaluating patients with suspected CS [75, 76]. In reality, both imaging modalities are complementary, and many patients require both CMR and cardiac [18F]FDG PET pending their clinical scenario.

In clinical practice, oftentimes the choice for initial testing is influenced by the clinician's clinical suspicion for CS. The joint SNMMI-ASNC expert consensus document outlines clinical situations in which high clinical suspicion for CS is raised and cardiac [18F]FDG PET/CT should be considered to assess evidence of active inflammation. The three major clinical scenarios include: patients with histologic evidence of extracardiac sarcoidosis and abnormal cardiac screening, young patients (< 60 years) with unexplained, new onset, significant conduction system disease, and patients with idiopathic sustained ventricular tachycardia [9]. However, even when the clinical diagnosis of CS is made based on the patient's clinical history and cardiac PET findings, clinicians may still find it helpful to have additional information from CMR as well, such as for evaluation of myocardial scar burden in a patient undergoing cardiac device placement to help guide decision-making. Similarly, even when CMR is positive for CS, cardiac [18F]FDG PET/CT is often still necessary to look for disease activity to help guide management.

Alternatively, in the clinical situation in which there is a lower suspicion for CS and/or the patient does not meet those predefined high-risk clinical features, such as a patient with unexplained dilated cardiomyopathy, proceeding with CMR as the initial test may be preferred given lack of ionizing radiation and the high negative predictive value of CMR for CS [58].

Combining CMR imaging with cardiac PET in the evaluation of patients with suspected CS offers a significant advantages in distinguishing CS from other similar conditions and capitalizes on the strength of CMR for detecting scar and PET for detecting disease activity. Furthermore, CMR provides morphological and structural information, and the distribution or pattern of LGE can indicate co-existing or alternative diagnoses [77].

Algorithm for PET and CMR imaging in patients with CS

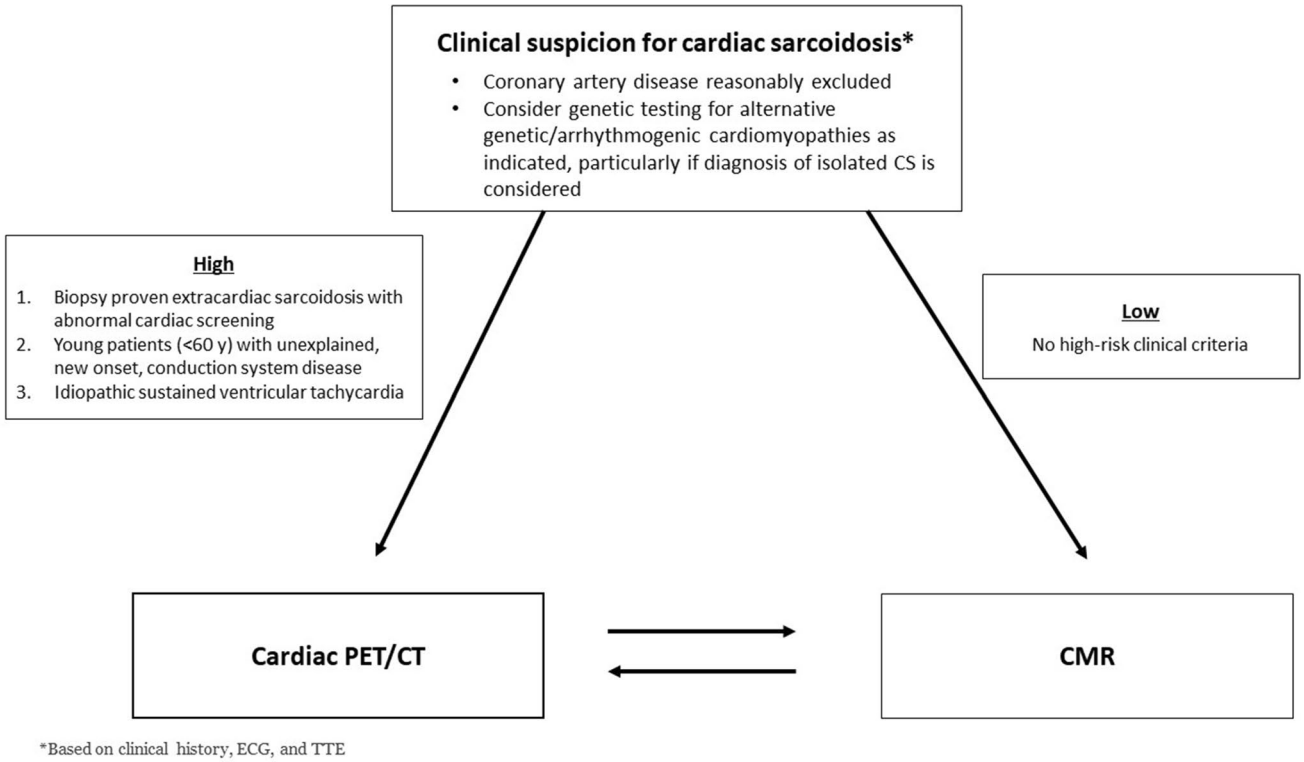

Unanswered issues and future directions

Future studies in CS should encompass not only advancements in the technical aspects of imaging modalities but also focus on enhancing the utilization of imaging by clinicians throughout the diagnostic and treatment processes. Serial imaging plays a crucial role in managing these patients; however, the ideal intervals for disease monitoring and surveillance are yet to be systematically evaluated. Moreover, additional research is needed to determine the optimal screening strategy and frequency for cardiac involvement in patients with extracardiac sarcoidosis, as well as to investigate whether early detection and treatment correlate with improved outcomes.

An optimal imaging modality for CS ideally combines the capabilities of myocardial scar detection through LGE on CMR and myocardial inflammation assessment via [18F] FDG uptake on cardiac PET/CT. Hybrid PET/MR imaging enables the co-registration of LGE CMR and cardiac [18F] FDG PET/CT images in a single scan, facilitating simultaneous detection of fibrosis and myocardial inflammation [78–80]. This approach has demonstrated improved diagnostic accuracy, with hybrid PET/MR achieving a sensivity of 94%, compared to 82% for CMR and 85% for cardiac PET/CT separately [81]. Simultaneous imaging also enhances the assessment of disease activity [79, 80] and prognosis, as combined abnormalities on CMR LGE and cardiac [18F] FDG PET/CT images have proven to be strong predictors of major adverse cardiac events [81, 82]. Furthermore, the addition of quantitative T1 and T2 mapping techniques to PET/MR imaging sequences contributes to the comprehensive assessment and diagnosis of patients [79, 82]. However, challenges such as higher costs and limited availability of hybrid scanners and experienced cardiac imagers proficient in the dual technique remain significant barriers to the routine clinical integration of hybrid PET/MR.

A significant challenge with PET imaging for CS is the requirement for complicated dietary preparation to suppress physiologic myocardial [18F]FDG uptake. Ongoing research focuses on developing novel PET tracers or new uses of existing tracers that eliminate the need for dietary preparation. Among the most promising candidates were the radiolabeled somatostatin analogs, particularly the ^{68}Ga-somatostatin analogs, which target multinucleated cells and activated macrophages that express somatostatin receptor (SSRT) 2 [83]. While initial results were promising,

a recent study suggests only moderate concordance beween [18F]FDG and a ^{68}Ga-somatostatin analog myocardial uptake [84]. More research in this area is needed.

Lastly, within the fields of cardiology and imaging, there are ongoing advancements in the integration of artificial intelligence (AI). However, the impact of AI on the diagnosis and management of patients with CS remains uncertain [85–87]. Further exploration is needed to understand the potential role of AI in enhancing CS diagnosis and patient care.

Conclusion

The increasing recognition of CS is largely attributed to advancements in cardiac imaging. Given the challenges associated with definitive diagnosis, including the absence of a reliable gold standard and the patchy nature of myocardial involvement, we heavily rely on advanced imaging for accurate diagnosis and effective treatment monitoring. [18F] FDG PET is the preferred modality for detecting active sarcoid lesions, identifying biopsy sites, and monitoring treatment response, while CMR demonstrates excellent negative predictive value and serves as the modality of choice for distinguishing CS from other cardiomyopathies. While the selection of advanced cardiac imaging modalities may vary based on local availability and expertise, adopting a multimodal imaging approach is paramount for the comprehensive diagnosis and management of cardiac sarcoidosis.

Declarations

Conflict of interest KA Young: nothing to disclose. T Raoult: nothing to disclose. L Leccisotti: nothing to disclose. BL Gerber: nothing to disclose. P Chareonthaitawee: nothing to disclose. O Gheysens: nothing to disclose.

Ethical approval This article does not contain any studies with human or animal subjects performed by any of the authors. All applicable international, national, and/or institutional guidelines for the care and use of animals were followed. All procedures performed in studies involving human participants were in accordance with the ethical standards of the institutional and/or national research committee and with the 1964 Helsinki declaration and its later amendments or comparable ethical standards. This article does not contain any studies with human participants performed by any of the authors.

Informed consent No humans were involved in this review article. Informed consent did not need to be obtained for this specific review.

References

1. Iannuzzi MC, Rybicki BA, Teirstein AS (2007) Sarcoidosis. N Engl J Med 357:2153–2165
2. Birnie DH, Nery PB, Ha AC et al (2016) Cardiac Sarcoidosis. J Am Coll Cardiol 68:411–421
3. Kandolin R, Lehtonen J, Airaksinen J et al (2015) Cardiac sarcoidosis: epidemiology, characteristics, and outcome over 25 years in a nationwide study. Circulation 131:624–632
4. Hulten E, Aslam S, Osborne M et al (2016) Cardiac sarcoidosis-state of the art review. Cardiovasc Diagn Ther 6:50–63
5. Silverman KJ, Hutchins GM, Bulkley BH (1978) Cardiac sarcoid: a clinicopathologic study of 84 unselected patients with systemic sarcoidosis. Circulation 58:1204–1211
6. Martusewicz-Boros MM, Boros PW, Wiatr E et al (2016) Prevalence of cardiac sarcoidosis in white population: a case–control study: proposal for a novel risk index based on commonly available tests. Medicine 2016:95
7. Kim RJ, Patel MR, Cawley PJ et al (2009) Detection of myocardial damage in patients with sarcoidosis. Circulation 120:1969–1977
8. Kouranos V, Tzelepis GE, Rapti A et al (2017) Complementary role of CMR to conventional screening in the diagnosis and prognosis of cardiac sarcoidosis. JACC Cardiovasc Imaging 10:1437–1447
9. Chareonthaitawee P, Beanlands RS, Chen W et al (2017) Joint SNMMI-ASNC expert consensus document on the role of 18F-FDG PET/CT in cardiac sarcoid detection and therapy monitoring. J Nucl Med 58:1341–1353
10. Cooper LT, Baughman KL, Feldman AM et al (2007) The role of endomyocardial biopsy in the management of cardiovascular disease: a scientific statement from the American Heart Association, the American College of Cardiology, and the European Society of Cardiology Endorsed by the Heart Failure Society of America and the Heart Failure Association of the European Society of Cardiology. Eur Heart J 28:3076–3093
11. Rosenbaum AN, Kolluri N, Elwazir MY et al (2021) Identification of a novel presumed cardiac sarcoidosis category for patients at high risk of disease. Int J Cardiol 335:66–72
12. Terasaki F, Yoshinaga K (2017) New guidelines for diagnosis of cardiac sarcoidosis in Japan. Ann Nucl Cardiol 3:42–45
13. Slart RHJA, Glaudemans AWJM, Lancellotti P et al (2017) A joint procedural position statement on imaging in cardiac sarcoidosis: from the Cardiovascular and Inflammation & Infection Committees of the European Association of Nuclear Medicine, the European Association of Cardiovascular Imaging, and the American Society of Nuclear Cardiology. Eur Heart J Cardiovasc Imaging 18:1073–1089
14. Birnie DH, Sauer WH, Bogun F et al (2014) HRS expert consensus statement on the diagnosis and management of arrhythmias associated with cardiac sarcoidosis. Heart Rhythm 11:1304–1323
15. Kumita S, Yoshinaga K, Miyagawa M et al (2019) Recommendations for 18F-fluorodeoxyglucose positron emission tomography imaging for diagnosis of cardiac sarcoidosis-2018 update: Japanese Society of Nuclear Cardiology recommendations. J Nucl Cardiol 26:1414–1433
16. Koiwa H, Tsujino I, Ohira H et al (2010) Images in cardiovascular medicine: imaging of cardiac sarcoid lesions using fasting cardiac 18F-fluorodeoxyglucose positron emission tomography: an autopsy case. Circulation 122:535–536
17. Lewis PJ, Salama A (1994) Uptake of fluorine-18-fluorodeoxyglucose in sarcoidosis. J Nuclear Med 1994:35
18. Slart RHJA, Glaudemans AWJM, Gheysens O et al (2020) Procedural recommendations of cardiac PET/CT imaging: standardization in inflammatory-, infective-, infiltrative-, and innervation-(4Is) related cardiovascular diseases: a joint collaboration of the EACVI and the EANM: summary. Eur Heart J Cardiovasc Imaging 21:1320–1330
19. Özütemiz C, Koksel Y, Froelich JW et al (2021) comparison of the effect of three different dietary modifications on myocardial

suppression in 18F-FDG PET/CT evaluation of patients for suspected cardiac sarcoidosis. J Nucl Med 62:1759–1767
20. Jamar F, Buscombe J, Chiti A et al (2013) EANM/SNMMI guideline for 18F-FDG use in inflammation and infection. J Nucl Med 54:647–658
21. Elwazir MY, Bird JG, AbouEzzeddine OF et al (2022) Performance of cardiac PET/CT with and without phase analysis for detection of scar in cardiac sarcoidosis: comparison to cardiac magnetic resonance imaging. J Nucl Cardiol 29:1389–1401
22. Kruse MJ, Kovell L, Kasper EK et al (2017) Myocardial blood flow and inflammatory cardiac sarcoidosis. JACC Cardiovasc Imaging 10:157–167
23. Sperry BW, Tamarappoo BK, Oldan JD et al (2018) Prognostic impact of extent, severity, and heterogeneity of abnormalities on 18F-FDG PET scans for suspected cardiac sarcoidosis. JACC Cardiovasc Imaging 11:336–345
24. Lobert P, Brown RKJ, Dvorak RA et al (2013) Spectrum of physiological and pathological cardiac and pericardial uptake of FDG in oncology PET-CT. Clin Radiol 68:59
25. Blankstein R, Osborne M, Naya M et al (2014) Cardiac positron emission tomography enhances prognostic assessments of patients with suspected cardiac sarcoidosis. J Am Coll Cardiol 63:329–336
26. Okumura W, Iwasaki T, Toyama T et al (2004) Usefulness of fasting 18F-FDG PET in identification of cardiac sarcoidosis. J Nucl Med 63:45
27. Yokoyama R, Miyagawa M, Okayama H et al (2015) Quantitative analysis of myocardial 18F-fluorodeoxyglucose uptake by PET/CT for detection of cardiac sarcoidosis. Int J Cardiol 195:180–187
28. Langah R, Spicer K, Gebregziabher M et al (2009) Effectiveness of prolonged fasting 18f-FDG PET-CT in the detection of cardiac sarcoidosis. J Nucl Cardiol 16:801–810
29. Tahara N, Tahara A, Nitta Y et al (2010) Heterogeneous myocardial FDG uptake and the disease activity in cardiac sarcoidosis. JACC Cardiovasc Imaging 3:1219–1228
30. Schildt JV, Loimaala AJ, Hippeläinen ET et al (2018) Heterogeneity of myocardial 2-[18F]fluoro-2-deoxy-D-glucose uptake is a typical feature in cardiac sarcoidosis: a study of 231 patients. Eur Heart J Cardiovasc Imaging 19:293–298
31. Miller RJH, Cadet S, Pournazari P et al (2022) Quantitative assessment of cardiac hypermetabolism and perfusion for diagnosis of cardiac sarcoidosis. J Nucl Cardiol 29:86–96
32. Osborne MT, Hulten EA, Singh A et al (2014) Reduction in ^{18}F-fluorodeoxyglucose uptake on serial cardiac positron emission tomography is associated with improved left ventricular ejection fraction in patients with cardiac sarcoidosis. J Nucl Cardiol 21:166–174
33. Ahmadian A, Brogan A, Berman J et al (2014) Quantitative interpretation of FDG PET/CT with myocardial perfusion imaging increases diagnostic information in the evaluation of cardiac sarcoidosis. J Nucl Cardiol 21:925–939
34. Waller AH, Blankstein R (2014) Quantifying myocardial inflammation using F18-fluorodeoxyglucose positron emission tomography in cardiac sarcoidosis. J Nucl Cardiol 21:940–943
35. Subramanian M, Swapna N, Ali AZ et al (2021) Pre-treatment myocardial 18FDG uptake predicts response to immunosuppression in patients with cardiac sarcoidosis. JACC Cardiovasc Imaging 14:2008–2016
36. Manabe O, Koyanagawa K, Hirata K et al (2020) Prognostic value of 18F-FDG PET using texture analysis in cardiac sarcoidosis. JACC Cardiovasc Imaging 13:1096–1097
37. Manabe O, Ohira H, Hirata K et al (2019) Use of 18F-FDG PET/CT texture analysis to diagnose cardiac sarcoidosis. Eur J Nucl Med Mol Imaging 46:1240–1247
38. Manabe O, Oyama-Manabe N, Nagai T et al (2020) Detailed visualization of the right and left ventricular, left atrial, and epicardial involvement of cardiac sarcoidosis with novel semiconductor PET/CT. Eur J Nucl Med Mol Imaging 47:1773–1774
39. Manabe O, Naya M, Aikawa T et al (2020) Recent advances in cardiac positron emission tomography for quantitative perfusion analyses and molecular imaging. Ann Nucl Med 34:697–706
40. Freeman AM, Curran-Everett D, Weinberger HD et al (2013) Predictors of cardiac sarcoidosis using commonly available cardiac studies. Am J Cardiol 112:280–285
41. Raftery EB, Oakley CM, Goodwin JF (1966) Acute subvalvar mitral incompetence. Lancet 2:360–365
42. Roberts WC, McAllister HA, Ferrans VJ (1977) Sarcoidosis of the heart. A clinicopathologic study of 35 necropsy patients (group 1) and review of 78 previously described necropsy patients (group 11). Am J Med 63:86–108
43. Smedema JP, van Geuns RJ, Ainslie G et al (2017) Right ventricular involvement in cardiac sarcoidosis demonstrated with cardiac magnetic resonance. ESC Heart Fail 4:535–544
44. Bruder O, Schneider S, Pilz G et al (2015) Update on acute adverse reactions to gadolinium based contrast agents in cardiovascular MR. Large multi-national and multi-ethnical population experience with 37788 patients from the EuroCMR registry. J Cardiovasc Magn Reson 17:1
45. Okasha O, Kazmirczak F, Chen KHA et al (2019) Myocardial involvement in patients with histologically diagnosed cardiac sarcoidosis: a systematic review and meta-analysis of gross pathological images from autopsy or cardiac transplantation cases. J Am Heart Assoc 2019:8
46. Pöyhönen P, Nordenswan H-K, Lehtonen J et al (2023) Cardiac magnetic resonance in giant cell myocarditis: a matched comparison with cardiac sarcoidosis. Eur Heart J Cardiovasc Imaging 24:404–412
47. Coleman GC, Shaw PW, Balfour PC et al (2017) Prognostic value of myocardial scarring on CMR in patients with cardiac sarcoidosis. JACC Cardiovasc Imaging 10:411–420
48. Messroghli DR, Moon JC, Ferreira VM, et al (2019) Clinical recommendations for cardiovascular magnetic resonance mapping of T1, T2, T2* and extracellular volume: a consensus statement by the Society for Cardiovascular Magnetic Resonance (SCMR) endorsed by the European Association for Cardiovascular Imaging (EACVI). J Cardiovasc Magn Reson 2017 :19. https://pubmed.ncbi.nlm.nih.gov/28992817/
49. Puntmann VO, Peker E, Chandrashekhar Y et al (2016) T1 mapping in characterizing myocardial disease: a comprehensive review. Circ Res [Internet] 119:277–299. https://pubmed.ncbi.nlm.nih.gov/27390332/
50. Tonegawa-Kuji R, Oyama-Manabe N, Aoki R et al (2021) T2-weighted short-tau-inversion-recovery imaging reflects disease activity of cardiac sarcoidosis. Open Heart. 8:00128
51. Greulich S, Deluigi CC, Gloekler S et al (2013) CMR imaging predicts death and other adverse events in suspected cardiac sarcoidosis. JACC Cardiovasc Imaging 6:501–511
52. Blankstein R, Waller AH (2016) Evaluation of known or suspected cardiac sarcoidosis. Circ Cardiovasc Imaging 9:3
53. Ahmadian A, Pawar S, Govender P et al (2017) The response of FDG uptake to immunosuppressive treatment on FDG PET/CT imaging for cardiac sarcoidosis. J Nucl Cardiol 24:413–424
54. Momose M, Fukushima K, Kondo C et al (2015) Diagnosis and detection of myocardial injury in active cardiac sarcoidosis-significance of myocardial fatty acid metabolism and myocardial perfusion mismatch. Circ J 79:2669–2676
55. Sgard B, Brillet PY, Bouvry D et al (2019) Evaluation of FDG PET combined with cardiac MRI for the diagnosis and therapeutic monitoring of cardiac sarcoidosis. Clin Radiol 74:81.e9-81.e18
56. Kim SJ, Pak K, Kim K (2020) Diagnostic performance of F-18 FDG PET for detection of cardiac sarcoidosis; a systematic review and meta-analysis. J Nucl Cardiol 27:2103–2115

57. Zhang J, Li Y, Xu Q et al (2018) Cardiac magnetic resonance imaging for diagnosis of cardiac sarcoidosis: a meta-analysis. Can Respir J 2018:586
58. Aitken M, Chan MV, Fresno CU et al (2022) Diagnostic accuracy of cardiac MRI versus FDG PET for cardiac sarcoidosis: a systematic review and meta-analysis. Radiology 304:566–579
59. Ning N, Guo HH, Iagaru A et al (2019) Serial cardiac FDG-PET for the diagnosis and therapeutic guidance of patients with cardiac sarcoidosis. J Card Fail 25:307–311
60. Vignaux O, Dhote R, Duboc D et al (2002) Clinical significance of myocardial magnetic resonance abnormalities in patients with sarcoidosis: a 1-year follow-up study. Chest 122:1895–1901
61. Flett AS, Hasleton J, Cook C et al (2011) Evaluation of techniques for the quantification of myocardial scar of differing etiology using cardiac magnetic resonance. JACC Cardiovasc Imaging 4:150–156
62. Ise T, Hasegawa T, Morita Y et al (2014) Extensive late gadolinium enhancement on cardiovascular magnetic resonance predicts adverse outcomes and lack of improvement in LV function after steroid therapy in cardiac sarcoidosis. Heart 100:1165–1172
63. Puntmann VO, Isted A, Hinojar R et al (2017) T1 and T2 Mapping in recognition of early cardiac involvement in systemic sarcoidosis. Radiology 285:63–72
64. Panovský R, Doubková M, Mojica-Pisciotti ML et al (2021) Left ventricular myocardial deformation assessment in asymptomatic patients with recently diagnosed sarcoidosis of the respiratory tract and/or extrapulmonary sarcoidosis. Orphanet J Rare Dis 2021:16
65. Dabir D, Meyer D, Kuetting D et al (2018) Diagnostic value of cardiac magnetic resonance strain analysis for detection of cardiac sarcoidosis. Rofo 190:712–721
66. Nakano S, Kimura F, Osman N et al (2013) Improved myocardial strain measured by strain-encoded magnetic resonance imaging in a patient with cardiac sarcoidosis. Can J Cardiol 29:1531.e9-1531.e11
67. Stevenson A, Bray JJH, Tregidgo L et al (2023) Prognostic value of late gadolinium enhancement detected on cardiac magnetic resonance in cardiac sarcoidosis. JACC Cardiovasc Imaging 16:345–357
68. Wang J, Zhang J, Hosadurg N et al (2023) Prognostic value of RV abnormalities on CMR in patients with known or suspected cardiac sarcoidosis. JACC Cardiovasc Imaging 16:361–372
69. Ahmed AI, Abebe AT, Han Y et al (2021) The prognostic role of cardiac positron emission tomography imaging in patients with sarcoidosis: a systematic review. J Nucl Cardiol 28:1545–1552
70. Tuominen H, Haarala A, Tikkakoski A et al (2019) 18F-FDG-PET in Finnish patients with clinical suspicion of cardiac sarcoidosis: female sex and history of atrioventricular block increase the prevalence of positive PET findings. J Nucl Cardiol 26:394–400
71. Zeppenfeld K, Tfelt-Hansen J, de Riva M et al (2022) 2022 ESC Guidelines for the management of patients with ventricular arrhythmias and the prevention of sudden cardiac death. Eur Heart J 43:3997–4126
72. Al-Khatib SM, Stevenson WG, Ackerman MJ et al (2018) 2017 AHA/ACC/HRS guideline for management of patients with ventricular arrhythmias and the prevention of sudden cardiac death: a report of the American College of Cardiology/American Heart Association Task Force on Clinical Practice Guidelines and the Heart Rhythm Society. Heart Rhythm 15:e73–e189
73. Kazmirczak F, Chen KHA, Adabag S et al (2019) Assessment of the 2017 AHA/ACC/HRS guideline recommendations for implantable cardioverter-defibrillator implantation in cardiac sarcoidosis. Circ Arrhythm Electrophysiol 2019:12
74. Athwal PSS, Chhikara S, Ismail MF et al (2022) cardiovascular magnetic resonance imaging phenotypes and long-term outcomes in patients with suspected cardiac sarcoidosis. JAMA Cardiol 7:1057–1066
75. Kebed KY, Carter SV, Flatley E et al (2021) Prevalence of newly diagnosed sarcoidosis in patients with ventricular arrhythmias: a cardiac magnetic resonance and 18F-FDG cardiac PET study. Int J Cardiovasc Imaging 37:1361–1369
76. Vita T, Okada DR, Veillet-Chowdhury M et al (2018) Complementary value of cardiac magnetic resonance imaging and positron emission tomography/computed tomography in the assessment of cardiac sarcoidosis. Circ Cardiovasc Imaging 11:e007030
77. Cummings KW, Bhalla S, Javidan-Nejad C et al (2009) A pattern-based approach to assessment of delayed enhancement in nonischemic cardiomyopathy at MR imaging. Radiographics 29:89–103
78. White JA, Rajchl M, Butler J et al (2013) Active cardiac sarcoidosis: first clinical experience of simultaneous positron emission tomography–magnetic resonance imaging for the diagnosis of cardiac disease. Circulation 2013:127
79. Greulich S, Gatidis S, Gräni C et al (2022) Hybrid cardiac magnetic resonance/fluorodeoxyglucose positron emission tomography to differentiate active from chronic cardiac sarcoidosis. JACC Cardiovasc Imaging 15:445–456
80. Dweck MR, Abgral R, Trivieri MG et al (2018) Hybrid magnetic resonance imaging and positron emission tomography with fluorodeoxyglucose to diagnose active cardiac sarcoidosis. JACC Cardiovasc Imaging 11:94–107
81. Wicks EC, Menezes LJ, Barnes A et al (2018) Diagnostic accuracy and prognostic value of simultaneous hybrid 18F-fluorodeoxyglucose positron emission tomography/magnetic resonance imaging in cardiac sarcoidosis. Eur Heart J Cardiovasc Imaging 19:757–767
82. Cheung E, Ahmad S, Aitken M et al (2021) Combined simultaneous FDG-PET/MRI with T1 and T2 mapping as an imaging biomarker for the diagnosis and prognosis of suspected cardiac sarcoidosis. Eur J Hybrid Imaging 2021:5
83. Saric P, Young KA, Rodriguez-Porcel M et al (2021) PET imaging in cardiac sarcoidosis: a narrative review with focus on novel PET tracers. Pharmaceut (Basel) 2021:14
84. Bravo PE, Bajaj N, Padera RF et al (2021) Feasibility of somatostatin receptor-targeted imaging for detection of myocardial inflammation: a pilot study. J Nucl Cardiol 28:1089–1099
85. Lu C, Wang YG, Zaman F et al (2022) Predicting adverse cardiac events in sarcoidosis: deep learning from automated characterization of regional myocardial remodeling. Int J Cardiovasc Imaging 38:1825–1836
86. Katsushika S, Kodera S, Nakamoto M et al (2021) Deep learning algorithm to detect cardiac sarcoidosis from echocardiographic movies. Circ J 86:87–95
87. Togo R, Hirata K, Manabe O et al (2019) Cardiac sarcoidosis classification with deep convolutional neural network-based features using polar maps. Comput Biol Med 104:81–86